SCIENCE CHINA
Technological Sciences

July 2010 Vol.53 No.7: 1847–1854
doi: 10.1007/s11431-010-3174-6

Study on peak overpressure and flame propagation speed of gas deflagration in the tube with obstacles

LUO JiaSong, WEI XiaoLin*, LI Sen, YU LiXin, ZHANG Yu, LI Teng & LI Bo

Institute of Mechanics, Chinese Academy of Sciences, Beijing 100190, China

Received January 2, 2010; accepted February 21, 2010

The on-way peak overpressure and flame propagation speed of gas deflagration in the tube with obstacles are important data for process safety. Based on carbon monoxide deflagration experiments, the paper presents a multi-zone integration model for calculation of on-way peak overpressure, in which the tube with obstacles is considered as a series of venting explosion enclosures which link each others. The analysis of experimental data indicates that the on-way peak overpressure of gas deflagration can be correlated as an empirical formula with equivalence ratio of carbon monoxide oxidation, expansion ratio, flame path length, etc., and that the on-way peak overpressure exhibits a linear relationship with turbulence factor and flame propagation speed. An empirical formula of flame propagation speed is given.

peak overpressure, flame propagation speed, obstacle, multi-zone integration model

Citation: Luo J S, Wei X L, Li S, et al. Study on peak overpressure and flame propagation speed of gas deflagration in the tube with obstacles. Sci China Tech Sci, 2010, 53: 1847–1854, doi: 10.1007/s11431-010-3174-6

1 Introduction

The main composition of converter off-gas is CO with little CO_2, O_2, and N_2, which is explosive [1]. During steelmaking, once the off-gas mixes with inhaled air and is ignited, the off-gas can deflagrate, and the deflagrating gas flow may propagate forward at more than hundreds m/s in the duct with obstacles. Deflagration is often accompanied with rapid increase of peak overpressure and flame propagation speed, and finally results in the serious damage to duct. Therefore, the study of peak overpressure and flame propagation speed during gas deflagration is very important to explosion suppression.

Deflagration involves chemical reaction, heat and mass transfer, turbulent flow, etc. Up to now, no suitable theoretical model has been used to predict the practical on-way peak overpressure (p) and flame propagation speed (S_F). Many experimental and numerical studies were conducted to investigate the influences of single factors (such as stoichiometric ratio (Φ), initial temperature (T_0), and initial pressure (p_0)) on the peak overpressure and flame propagation speed of deflagration [2–5]. Silvestrini et al. [6] studied the calculation formulae of the peak overpressure and flame propagation speed of deflagration by theoretic analyses, but the formulae were complex and not practical, in which turbulent fluctuation velocity should be given.

The theory of vented explosion of single chamber is relatively suitable, and it can predict the peak overpressure of deflagration at given geometric condition and the basic combustion velocity [7]. Cubbage and Simmonds [8] provided a simple vented explosion model:

$$p_{\mathrm{red}} = 0.365\left(\frac{\overline{A}}{\overline{S_0}}\right)^{-1},$$

where $\overline{A} = \dfrac{C_d A_V}{A_s}$; C_d is flow coefficient; A_V is the opening

*Corresponding author (email: xlwei@imech.ac.cn)

area of chamber, m^2.

$$\overline{S_0} = \frac{S_{u0}}{c_0}\left(\frac{\rho_{u0}}{\rho_{b0}} - 1\right) = \frac{S_{u0}}{c_0}(E_0 - 1),$$

where S_{u0} is the basic combustion velocity, m/s; c_0 is sound velocity, m/s; $E_0 = \rho_u / \rho_b$; ρ_u is the density of the unburned gas, kg/m^3; ρ_b is the density of the burning gas, kg/m^3 . Park et al. [9] used the vented explosion model to calculate each peak overpressure of two chambers separated by obstacle (ignition chamber and after-obstacle chamber). p_{red1} is the peak overpressure of basic vented explosion in the ignition chamber. The peak overpressure of the entire system is the peak overpressure of the after-obstacle chamber, which consists of three components: (1) The basic peak overpressure of vented explosion of the after-obstacle chamber (p_{red2}); (2) the pressure of after-obstacle chamber transfered by the basic peak overpressure of vented explosion in the ignition chamber, $\frac{(p_{\text{red1}} + p_a)}{p_a}$; (3) pressure correction term related with geometric condition and turbulence, $C = \exp\left[a\left(VBR\frac{L_f}{D_0}\right) + b\left(A_x^{0.5}\frac{L}{D}\right) + c\left(C_D\frac{\overline{S_F}}{S_L}\right) + d\right]$. Therefore, the peak overpressure in the after-obstacle chamber can be expressed as

$$p_{\text{red}} = p_{\text{red2}}\frac{(p_{\text{red1}} + p_a)}{p_a}C .$$

However, the method established by Park is not suitable for the peak overpressure calculation of duct with obstacles. The method is only suitable for the two bonding chambers, not for long duct. In addition, the statement about the effect of turbulent in the expression $\left(\frac{\overline{S_F}}{S_L}\right)$ can not be directly calculated, and the average turbulence flame propagation speed needs to be determined by experiments.

In the paper, based on the work of Park et al. [9], a multi-zone integration model is presented for the calculation of on-way peak overpressure; the tube with obstacles is considered as a series of venting explosion enclosures which link each others. The model only involves the stoichiometric ratio of mixed gas, initial temperature, and geometric conditions of duct. The formulae of on-way peak overpressure and flame propagation speed of deflagration (S_F) are correlated, which are expressed by known variables, not by unknown variables (such as turbulent velocity). Therefore, the on-way peak overpressure and flame propagation speed of deflagration of carbon monoxide can be directly calculated by the established formulae.

2 Experimental system and procedure

An experimental system is set up for investigating relationship between peak overpressure and flame propagation speed and their respective impact factors during deflagration in the tube with obstacles. As shown in Figure 1, the system mainly consists of two parts, experimental apparatus and data processing system.

2.1 Experimental apparatus

A Roots blower driven by frequency converter is used to pump air via a thermal mass flow meter (TMF) and airflow is then divided into two streams. One stream enters the humidification section, which passes through a water tank, and then mixes with another stream. Ball valves are set in both air stream tubes for regulating the ratio of both airflows. A hygrothermograph is fixed at the end of humidification section to measure air humidity and temperature of mixed flow. The relative humidity of the mixed air is 62%. Then the mixed air flows into the electric heater and is heated to a certain temperature. The temperature of heater can be set down on control panel, and thus the temperature of the airflow fed to the test section could be adjusted. CO is provided by gas bottles with pressure regulator. The flow rate of the CO is controlled by a mass flow controller (MFC). Air and CO gas are mixed thoroughly before the entrance of test section and then ignited by electric spark, The nominal ignition energy is about 20 J. Thermal couples are mounted at the front and rear of the igniter to measure the temperature of the premixed gas both before-ignition and after-ignition.

The test section is a horizontal semi-open deflagration tube of 5.26 m in length from igniter to outlet, and inner de diameter is 0.08 m. The tube consists of an empty section without obstacles of 2.76 m in length and a section with obstacles of 2.5 m in length. The obstacle is assembled by

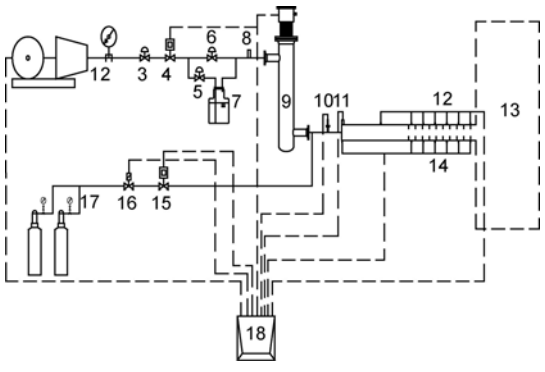

1, Roots blower driven by frequency converter; 2, air pressure gauge; 3, ball valve; 4, thermal mass flow meter; 5, ball valve 6 ball valve; 7, water tank; 8, sampling port of hygrothermograph; 9, electric heater; 10, thermal coupler; 11, igniter; 12, pressure transducers; 13, quieter; 14, flame sensors; 15, mass flow controller; 16, electromagnetic valve; 17, gas bottles; 18, console and data processing system.

Figure 1 The experimental system.

10 identical rings spaced 0.2 m apart. The blockage ratio of the ring is defined as *BR* = blocking area of obstacle/cross-section area of deflagration tube. Here *BR*=1 $(d/D)^2$=0.4375, where the inner diameter of tube *D*=0.08 m and orifice diameter of ring *d*=0.06 m. Because of the toxicity of CO and the loud noise made by deflagration which could reach up to 125 dB, an exhaust equipment with a quieter is installed at the outlet of deflagration tube.

2.2 Data processing system

Seven pressure transducers and seven flame sensors are placed at locations along the deflagration tube shown in Figure 2. Pressure transducers are numbered from 1 to 7 and flame sensors are numbered from 8 to 14. Pressure transducer No.8 locates at the place of ignition for confirming the time of catching fire. Pressure transducers 2–7 are located along the tube in one-to-one correspondence with the pressure transducers 9–14 for research of relationship between light signals of flame and pressure signals. All the 14 electrical signals are amplified and then collected by a dynamic high-speed data acquisition system (DHDAS5939) with sampling frequency of 500 kHz. Finally, the digital signals are transferred to computer by IEEE-1394 FireWire cable.

The experiments are performed by operating the console. Several parameters, such as air/CO ratio, temperature of electric heater, temperature of premixed gas and the ignition of electric spark are controlled with different experimental settings. Figure 3 is the typical overpressure profiles and flame photoelectric voltage profiles in time at four locations along the tube during deflagration. Figure 3(a) shows the overpressure profiles in time (*p*-*t* chart), and each curve in chart represents the variation of overpressure at one location. Figure 3(b) shows flame photoelectric voltage profiles in time (*U*-*t* chart), and each curve represents the variation of flame photoelectric voltage at one location.

The peak overpressure and the time (t_i) corresponding to rising edges of flame photoelectric voltage at each location along the tube can be obtained directly from the test data. Once the distance (*L*) of every two measurement locations is measured, the average flame propagation speed among the locations can be calculated by using expression $S_{Fi} = \dfrac{L}{t_i - t_{i-1}}$. And thus the flame propagation speed at each location could be obtained by interpolation.

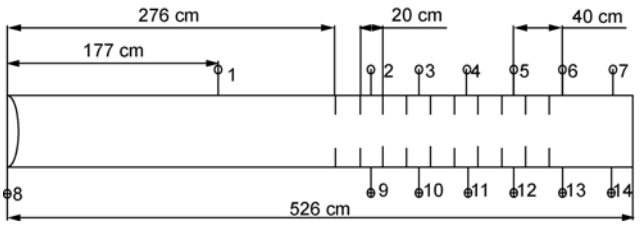

Figure 2 Locations of pressure transducers and flame sensors.

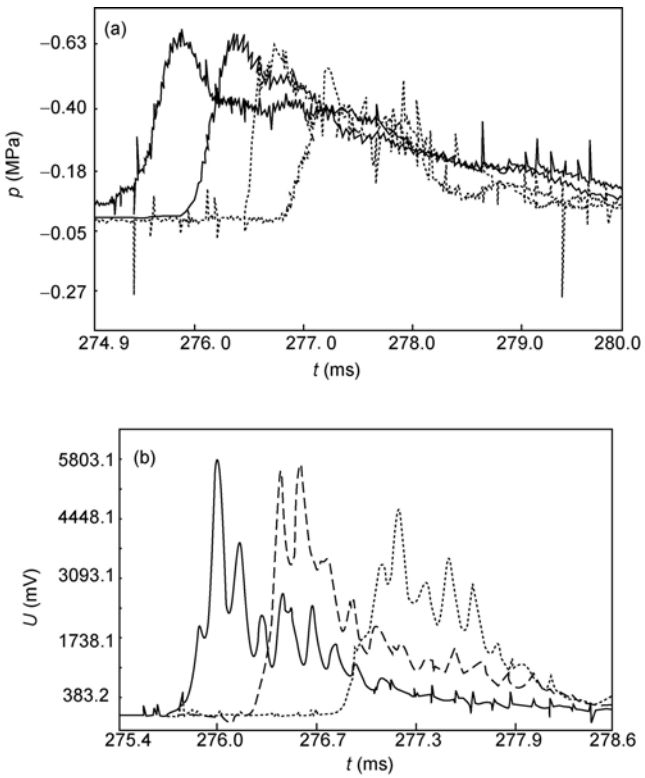

Figure 3 Overpressure profiles and flame photoelectric voltage profiles in time. (a) *p*-*t* chart; (b) *U*-*t* chart.

Deflagration experiments were conducted for 44 times with different equivalent ratios of CO/air (Φ) and different temperatures of premixed gas. In each condition, 7 overpressure profiles and 7 flame photoelectric voltages profiles with time were recorded, therefore 6 flame propagation speed values along the tube could be calculated in every experiment. For the pressure transducers No.1 and No.7 locate at the section without obstacles, the study focused on the data process of the overpressure values measured by pressure transducers No.2–No.6.

3 Multi-zone integration model and data processing methods

A multi-zone integration model is proposed in the paper, which treats the tube with internal obstacles as a series of adjacent cells. The peak overpressure (p_1) in the first cell is calculated using the peak overpressure of venting explosion enclosures. The peak overpressure (p_i) in the sequent cell is determined by both the peak overpressure (p_{i-1}) of the upstream adjacent cell and local parameters. Continuously, the overpressure profiles can be calculated and the formula is given.

Figure 4 shows the sections of the tube. The peak overpressure of one cell is determined by the upstream adjacent peak overpressure, local ratio of fuel to air, local temperature

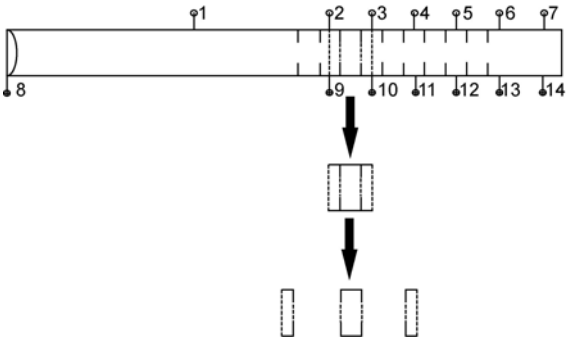

Figure 4 Tube with obstacles seperated by multi-zones.

and other local geometrical parameters. Multi-zone integration model combines explosion theory and peak overpressure calculation together, which outputs the peak overpressures by only inputting the geometrical parameters of the cell and the chemical parameters of the mixture gas there. The whole methodology is illustrated in Figure 5. Firstly, adding the adjacent upstream peak overpressure (p_{i-1}) and other terms containing the ratio of fuel to gas (Φ) and the flame propagation speed (S_F) to build an initial calculation formula. Secondly, adjust the parameters of all those terms to fit the calculations to the experimental data, and to make the calculation errors the smallest. Finally, the optimal formula is collected.

The coefficient of the formula is determined through minimizing the sum of squares of the difference between experimental data and calculated data (e_{squ}) or the sum of absolute values of the difference (e_{abs}).

$$e_{\text{squ}} = \frac{\Sigma(p_{\text{cal}} - p_{\text{exp}})^2}{\Sigma p_{\text{exp}}^{\ 2}}, \tag{1}$$

$$e_{\text{abs}} = \frac{\Sigma\left|p_{\text{cal}} - p_{\text{exp}}\right|}{\Sigma\left|p_{\text{exp}}\right|}. \tag{2}$$

By means of mathematical program MATLAB, the minimum value can be obtained for the optimized parameters e_{squ} (or e_{abs}). And then the other uncertain parameters are obtained. In calculations, the least-squares method is used for seeking the smallest errors of the multi-zone integration model, whose stability is good and easy to get better uncertain parameters. After the parameters are determined, the absolute value of error is calculated as a reference.

4 Analysis of experimental results

4.1 The expression of peak overpressure

Figure 6 shows the effects of equivalent ratio of CO/air,

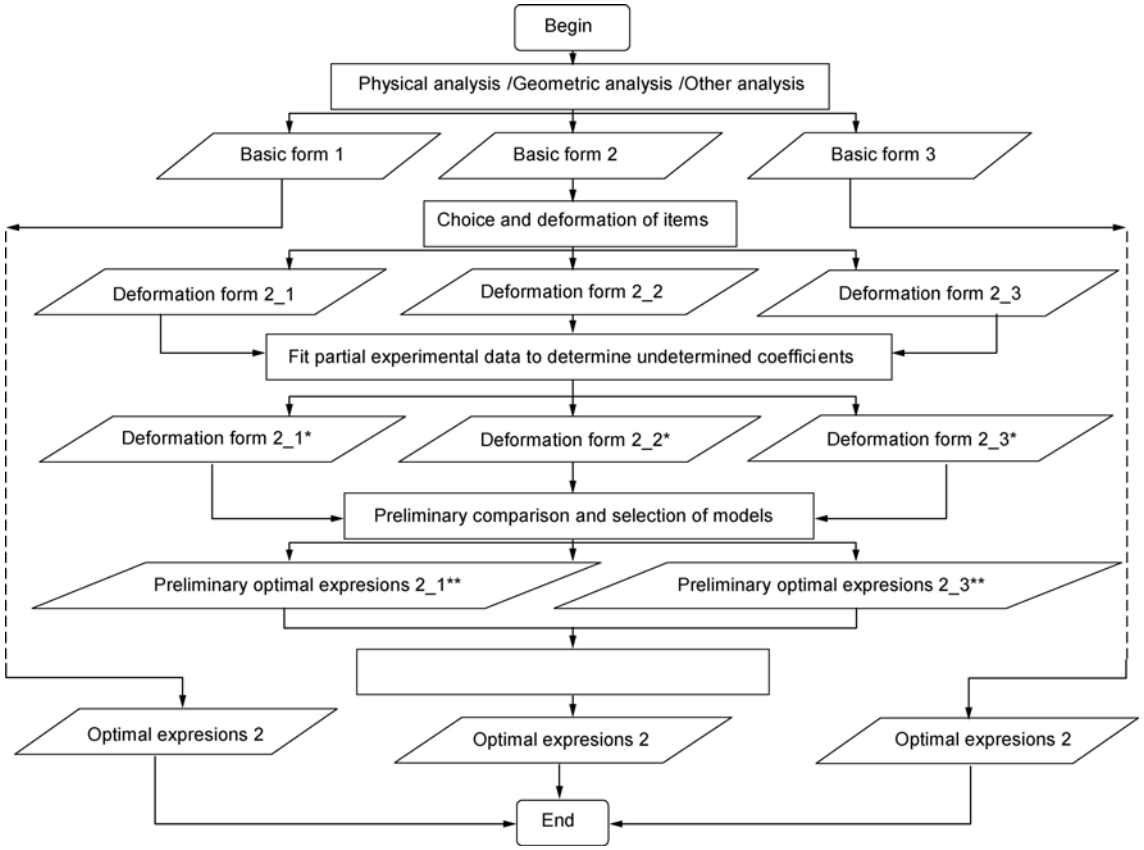

Figure 5 Flow chart of data analysis.

initial temperature, and flame path length on the peak overpressures. Figure 6(a) indicates the relationship between on-way peak overpressure (p_i/p_a) and equivalent ratio of CO/air (Φ). In the figure, No.1–No.7 represents the pressure detectors set along the test tube. The peak overpressure firstly increases and then decreases with increasing the CO ratio. The tendency might be expressed by a parabola function. Figure 6(b) shows that as the expansion ratio (E_0) increases the peak overpressure (p_i/p_a) almost linearly increases. Figure 6(c) demonstrates the relationship between on-way peak overpressure (p_i/p_a) and the flame path length (L_f/D). The points in each curve represent the peak overpressure values measured by the pressure detectors (1–7) under certain temperature. When the data processing focuses on the points of 2–6, the curve shows that the peak overpressure also increases almost linearly as the flame path length increases. Therefore, $\frac{p_i}{p_a}$ can be expressed as a linear function of the following terms: $(\Phi - f)^2$, E_0, and L_f/D.

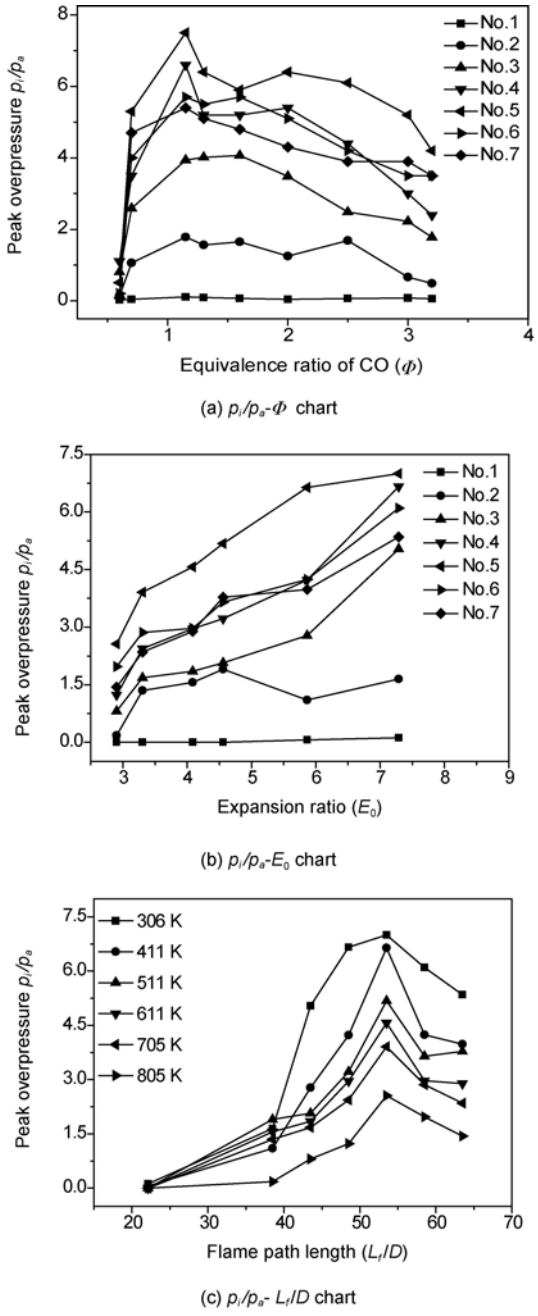

Figure 6 Effects of equivalent ratio of CO/air and flame path length on the peak overpressure. (a) p_i/p_a-Φ chart; (b) p_i/p_a-E_0 chart; (c) p_i/p_a -L_f/D chart.

During the correlation, some terms may be added or deleted based on the linear expression. If the term decreases the error, it needs to be remained. But if it increases the error, it is unwanted. Deleting a certain term in the linear expression equals to replace it by a constant. If the error becomes small after deleting it, it will be a term with small sensitivity. Except the linear expression, multiplying some term or its power is also used. Finally, more than ten expressions are correlated.

After selection, the following formula is determined as the optimal expression:

$$\frac{p_i}{p_a} = a\frac{p_{i-1}}{p_a} + b(\Phi - f)^2 + cE_0 + d\frac{L_f}{D} + e, \tag{3}$$

where p_i is the unknown peak overpressure (i=2, 3, 4, 5, 6). P_a is the atmosphere pressure. p_{i-1} is the upstream adjacent peak overpressure. The peak overpressure in the first cell (p_1) is calculated by a vented explosion expression: $p_{\mathrm{red1}} = \left(\frac{\overline{A_1}}{S_0}\right)^{-1}$. Φ is the equivalent ratio of CO/air. $E_0 = T_{\max}/T_0 = \rho_u/\rho_b$ is the expanding ratio. L_f/D is the non-dimensional length of flame. D is the diameter of the tube. A, b, c, d, e and f are uncertain parameters.

After calculations, the best parameters of eq. (3) are a=0.8275; b=0.1324; c=0.168; d=4.186; e=1.6936; f=1.60.

The ranges of the variables are Φ=0.7–3.2, E_0=2.9–7.5, and L_f/D=42.9–57.9.

Figure 7 gives the comparison of the experimental results to the predicted results, and it can be seen that the predictions are in good agreement with the experimental data.

From calculations, the followings can also be concluded.

As what suggested by Park [9], an additional term $\frac{p_{i-1} + p_a}{p_a}$ was added in eq. (3), but the calculation accuracy was not obviously increased. An exponential function was used for calculating E_0 term, but the predictions were even worse. It has been proved by many tests that eq. (3) is the best formula of the peak overpressure. Arranging those terms in eq. (3) in descending of importance, the sequence is $p_{i-1}/p_a > (\Phi - f)^2 > (L_f/D) > E_0$. For the formula with the less

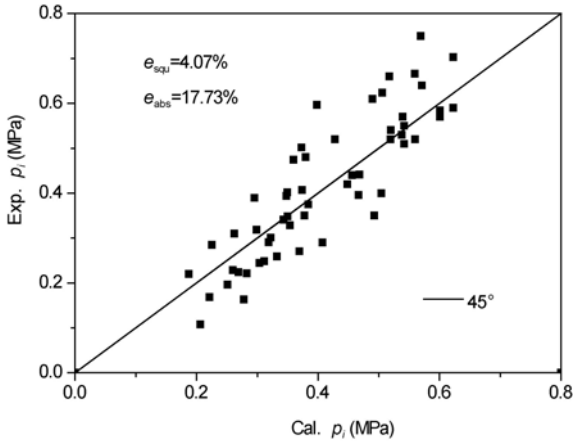

Figure 7 Comparison between experimental data and calculated data by eq. (3).

error, the value of f can be calculated stably and obtained as f=1.5–1.9. When the other conditions are not changed, the peak overpressure attains higher at $\Phi=f$, corresponding to the fundamental combustion experimental results by Frassoldati et al. [10].

4.2 The relationship of peak overpressure and flame propagation speed

The peak overpressure of gas deflagration can be predicted by eq. (3), but the flame propagation speed is still not obtained. By the model of Park [9], the primary relation between peak overpressure and flame propagation speed may be expressed as

$$\frac{p_i}{p_a}=\left(\frac{p_{\mathrm{red}\_i}}{p_a}\right)\left(\frac{p_{i-1}+p_a}{p_a}\right)\left(a\frac{S_{Fi}}{S_L\cdot E}+b\right), \tag{4}$$

where p_i is peak overpressure at i section, p_{red_i} is basic peak overpressure of vented explosion, p_{i-1} is peak overpressure at i–1 section, and p_a is atmosphere pressure.

The first term in the right side of eq. (4) is the basic term of vented explosion, for which different models of vented explosion can be used. The second term is the successive pressure term, which is relative with the calculated peak overpressure in the former section. The third term is the turbulent corrected term, and the term $\frac{S_{Fi}}{S_L\cdot E}$ stands for turbulent factor, where $E=(E_0-1)(\frac{p}{p_0})^{-(1-1/\gamma)}+1$ [6]. Silvestrini [6] indicates that $S_F=S_TE$ when some conditions can be satisfied. Since turbulence factor $\beta=\frac{S_T}{S_L}$, the term $\frac{S_{Fi}}{S_L\cdot E}$ is β, may stand for the effect of turbulence.

Through the process of choice and transformation, more than ten formulae can be induced. Compared with these formulae, the following results may be given.

The different peak overpressure terms of vented explosion will increase the error of the expression, which may be deleted. The term $\frac{p_{i-1}+p_a}{p_a}$ will make the formulae complicated and increase the error, which may be deleted. Adding new exponent factor, for example in E_0, will also increase the error.

Through a round of choices, the optimal formula can be determined as

$$\frac{p_i}{p_a}=a\frac{S_{Fi}}{S_L\cdot E}+b, \tag{5}$$

where a=0.008245; b=1.478.

The range of independent variable is $\frac{S_{Fi}}{S_L\cdot E}$ = 45.0–71.9.

From eq. (5), it can be seen that the peak overpressure increases with the enhancement of turbulent factor. Figure 8 indicates the comparison between experimental data and calculated data by eq. (5), and both agree with well.

4.3 The expression of flame propagation speed

The peak overpressure in gas deflagration can be predicted by eq. (3) through substituting the known independent variables. And the relationship between peak overpressure and flame propagation speed has been given by eq. (5). Substituting eq. (3) into eq. (5), the flame propagation speed S_F can be expressed by the known variables (Φ, E_0, etc.) as

$$\begin{aligned}\frac{S_{Fi}}{S_L}&=\frac{E}{a'}\left(\frac{p_i}{p_a}-b'\right)\\&=\frac{E}{a'}\left[\left(a\frac{p_{i-1}}{p_a}+b(\Phi-f)^2+cE_0+d\frac{L_f}{D}+e\right)-b'\right],\end{aligned} \tag{6}$$

where the value ranges of a, b, c, d, e, f are the same as those in Section 3.1. In addition, a'=0.008245, b'=1.478.

The range of independent variable is E=2.38–6.65, Φ=0.7–3.2, E_0=2.9–7.5, L_f/D=42.9–57.9. Figure 9 indicates the comparison between experimental data and calculated data by the eq. (6), and both agree with well.

5 Discussion of the applicability of the formula

Yu et al. [11, 12] conducted many gas deflagration experiments. The tube size is diameter D = 0.08 m, length L = 5 m, blockage ratio BR = 0.438, and equivalence ratio Φ = 0.58. H_2, C_2H_2, CH_4, and water gas were used. To correlate the data, the experimental data were in good agreement with the predictions by eq. (3), as shown in Figure 10.

Certainly, the coefficients in eq. (3) are different for various gases, but the linear expression can get good fitting result for experimental data.

Similarly, the results of flame propagation speed predicted by eq. (6) were compared with the experimental data as shown in Figure 11.

6 Conclusions

Gas deflagration experiments were conducted in the tube with obstacles, in which the humidity, temperature, and equivalence ratio of mixing gas could be controlled. Through the fitting method, the experimental data were correlated and the optimal formulae were presented. The following conclusions are drawn by the analysis.

(1) $\frac{p_i}{p_a}$ can be expressed as a linear function of the known variables: $\frac{p_{i-1}}{p_a}$, $(\Phi - f)^2$, E_0, and L_f/D. The calculation values of $\frac{p_i}{p_a}$ are in good agreement with experimental data.

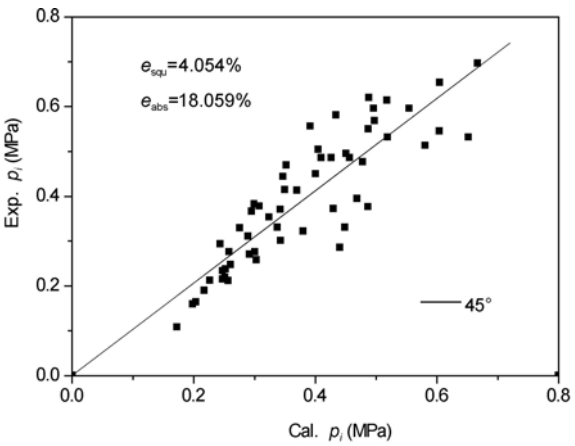

Figure 8 Comparison between experimental data and calculated data by eq. (5).

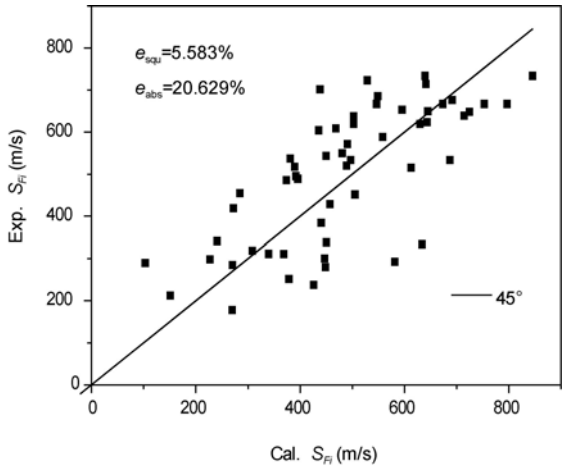

Figure 9 Comparison between experimental data and calculated data by the expression of S_F.

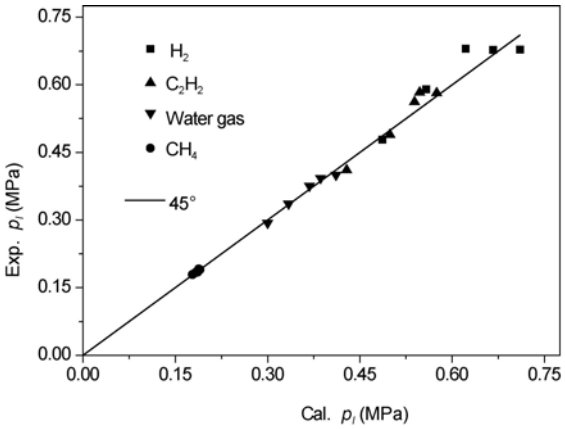

Figure 10 Comparison between experimental data by Yu et al. [11, 12] and the calculated data by eq. (3).

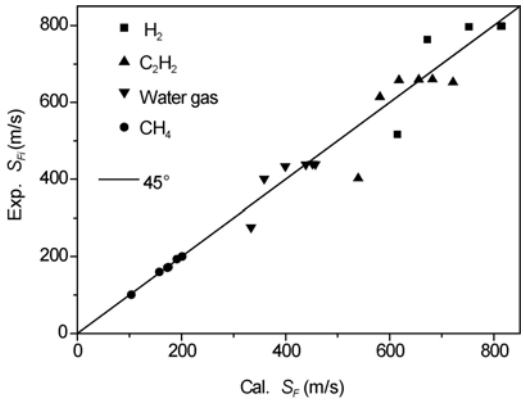

Figure 11 Comparison between experimental data by Yu, et al. [11, 12] and the calculated data by eq. (6).

In experiments, the order of significance of the factors is as follows: $p_{i-1}>(\Phi-f)^2>(L_f/D)>p_{red\_i}>E_0$. In the term $(\Phi-f)^2$, f=1.5–1.9. When the other conditions are not changed, the peak overpressure attains higher at $\Phi=f$.

(2) Under the condition that obstacles are uniform, $\frac{p_i}{p_a}$ and $\frac{S_{Fi}}{S_L \cdot E}$ approximately present the simple linear relationship when $\frac{S_{Fi}}{S_L \cdot E}$=45.0–71.9. This means the value of peak overpressure increases linearly with the enhancement of turbulence intensity.

(3) The calculated values of flame propagation speed can be obtained by the linear expression of known variables $\frac{p_{i-1}}{p_a}$, $(\Phi-f)^2$, (L_f/D), E_0, which are in good agreement with experimental data.

This work was supported by the National Natural Science Foundation of China (Grant No. 50976122), the National Hi-Tech Research and Development Program of China ("863" Program) (Grant No. 2006AA05Z253), and the Knowledge Innovation Program of the Chinese Academy of Sciences (Grant No. KGCX2-YW-321), The authors would like to thank Zhang Liang, Huang Xueliang, and Zhan Huanqing for their help.

1 Gao Z P. Steel-making Technology. Beijing: Metallurgical Industry Press, 2006
2 Oh K H, Kim H, Kim J B, et al. A study on the obstacle-induced variation of the gas explosion characteristics. J Loss Prev, 2001, 14: 597–602
3 Ibrahim S S, Hargrave G K, Williams T C. Experimental investigation of flame/solid interactions in turbulent premixed combustion. Exp Therm Fluid Sci, 2001, 24: 99–106
4 Ibrahim S S, Masri A R. The effects of obstructions on overpressure resulting from premixed flame deflagration. J Loss Prev, 2001, 14: 213–221
5 Salzano E, Marra F S, Russo G, et al. Numerical simulation of turbulent gas flames in tubes. J Hazard Mater, 2002, 95: 233–247
6 Silvestrini M, Genova B, Leon F J. Correlations for flame speed and explosion overpressure of dust clouds inside industrial enclosures. J Loss Prev, 2008, 21: 374–392
7 Razus D M, Krause U. Comparison of empirical and semi-empirical calculation methods for venting of gas explosions. Fire Saf J, 2001, 36: 1–23
8 Cubbage P A, Simmonds W A. An investigation of explosion reliefs for industrial drying ovens. Trans Inst Gas Eng, 1955, 105: 470–475
9 Park D J, Lee Y S, Green A R. Prediction for vented explosions in chambers with multiple obstacles. J Hazard Mater, 2008, 155: 183–192
10 Frassoldati A, Faravelli T, Ranzi E. The ignition, combustion and flame structure of carbon monoxide/hydrogen mixtures. Note 1: Detailed kinetic modeling of syngas combustion also in presence of nitrogen compounds. Int J Hydrog Energy, 2007, 32: 3471–3485
11 Yu L X, Sun W C, Wu C K. Influence of obstacle-produced turbulence on development of premixed flames. Sci China Ser E-Tech Sci, 2002, 45: 184–194
12 Yu L X, Sun W C, Wu C K. Flame acceleration and overpressure development in a semiopen tube with repeated obstacles. Proc Combust Inst, 2002, 29: 321–327